Silicon (2024) 16:3431–3451
https://doi.org/10.1007/s12633-024-02884-2

RESEARCH

Study of Correlation of Machining Performance and Geometrical Tolerances of Si_3N_4-TiN Composites Using EDM Process

K. P. Manikandan[1] · S. Thirugnanam[1] · L. Selvarajan[2] · T. S. Senthilkumar[3]

Received: 20 November 2023 / Accepted: 30 January 2024 / Published online: 5 March 2024

Abstract

The aim of this research work is to enhance the machining characteristics and geometrical tolerances of Si_3N_4–TiN ceramic composite using a copper electrode as the EDM tool. The investigation encompassed a comprehensive exploration of various machining parameters, including polarity, current (amp), pulse on time (µs), pulse off time (µs), dielectric pressure (Kg/cm^2), gap voltage (v), spark gap (mm), and servo speed (m/s), utilizing a Taguchi L_{18} orthogonal array. Throughout the EDM process, meticulous scrutiny was applied to output characteristics such as Material Removal Rate (0.0354 gm/min), Tool Wear Rate (0.001035 gm/min), Wear Ratio (22.625), Surface Roughness (0.117 µm), Top Radial Overcut (0.043 mm), Bottom Radial Overcut (-0.214 mm), top diameter of the drilled hole (5.087 mm), bottom diameter of the drilled hole (4.572 mm), Taper Angle (0.458 deg), Circularity (0.039 mm), Cylindricity (0.034 mm), Perpendicularity (0.007 mm), and Run Out (0.036 mm). The higher pulse current promotes the formation of a stable plasma channel which results in increasing the material removal rate. The improved flushing action helps to minimize the recast layer, leading to a smoother surface finish and reduced surface roughness. The experimental results demonstrate that as the spark gap increases from 0.18 mm to 0.25 mm, the Runout, Electrode Wear Rate, ROC Bottom, ROC Top, and Taper Angle drastically reduce.

Keywords Ceramic composite · CIR · CYL · PER · RO

1 Introduction

Very few machinability research on conductive ceramics have been reported, according to the thorough literature search that was done. Non-conductive ceramics are high-temperature materials with a variety of applications, thus they require careful consideration when being processed with an EDM. Electrical discharge machining (EDM) involves heating the material to a point where it melts and evaporates, converting electrical energy into thermal energy. Upon impact with the dielectric, the molten material either forms a crater or is eroded into debris. Some examples of external factors that greatly affect the result include cryogenic treatment and hardening.Computational and mathematical modelling of the EDM process allows for the optimisation of technical parameters in combination with empirical data to achieve the required surface quality of the work piece while minimising flaws [1].

Not all of the EDM processing's facets that influence performance characteristics are covered in the scant literature that is currently in existence. Intermetallic/ceramic composites made of $MoSi_2$ and SiC have earned a reputation as excellent engineering materials for high-temperature and hazardous situations [2]. $MoSi_2$-SiC ceramics have been used in filters, gas turbine blades, engines in the aerospace industry, shrouds and combustor liners, and other applications due to its high resistance, low down density, and powerful electric conductivity [3].

✉ K. P. Manikandan
manikandanp.mech@srmvalliammai.ac.in

S. Thirugnanam
thirugnanams.mech@srmvalliammai.ac.in

L. Selvarajan
selvalakshmanan86@gmail.com

[1] Department of Mechanical Engineering, SRM Valliammai Engineering College (Autonomous), Chengalpattu District 603203, Tamilnadu, India

[2] Department of Mechanical Engineering, Mahendra Institute of Technology (Autonomous), Namakkal District, Tamilnadu 637 503, India

[3] Department of Mechanical Engineering, K. Ramakrishnan College of Technology, Tiruchirappalli 621 112, Tamilnadu, India

Electrical Discharge Machining, involves heating material to a melting point through electrical energy, converting it to thermal energy. The molten substance either forms a crater or is washed away when contacting the dielectric. Extrinsic factors like hardening and cryogenic treatment impact outcomes. Optimizing parameters using empirical data and numerical modeling enhances surface quality while minimizing defects. Electrically conductive ceramics and diverse electrode materials, such as composite-based, copper, tungsten carbide, aluminum, and copper tungsten, advance EDM. Non-electrical factors like work-piece and tool material rotation, along with dielectric fluid flushing, influence EDM performance metrics [4].

The complexity of these materials necessitates the use of time-consuming, expensive classical machining methods to manufacture intricate structures, which result in fissures on the machined surface [5]. It also has poor machinability and creates constructions with built-up edges. As a result, the cutting tool degrades throughout the machining procedure, requiring the purchase of an expensive tool. In the end, electric discharge machining is believed to be the most effective technique for cutting ceramic composites. It has been established that the EDM method is the best approach for machining ceramic-based composites since there is no mechanical connection between the tool electrode and the material of the work piece [6].

The material removal rate (MRR), tool wear rate (TWR), and surface finish are a few of the output characteristics that various academics have attempted to optimize and investigate the impact of various machining parameters [7]. To obtain a lower MRR, efforts have been focused more on the spark EDM process and the machining of any electrically conducting components. To increase MRR in spark EDM, ceramic composites have been machined using EDM paired with a solid electrode [8].Therefore, an effort is made in the current work to select an appropriate unconventional method for electric discharge machining of conductive ceramic composites.

Since $MoSi_2$-based composite materials exhibit great flexible modulus and brilliant oxidation resistance at an extraordinarily high temperature of 1800 °C under oxidizing and forceful conditions, they are regarded as expected fundamental ceramics [9]. Due to the development of a stable silicon dioxide layer on its surface at high temperatures, $MoSi_2$ is a conductive silicide with oxidation resistance [10].

An effort is made in the author's present research to identify a suitable electrode material for EDM of intermetallic ceramic composites. Aluminum, copper, tungsten, carbide, and brass are examples of materials with low melting points that work well for EDM when using metallic electrodes [11]. In light of the higher-than-average frequencies anticipated for EDM, metallic electrodes like copper are advised [12]. Since it performs better in discharge dressing to function at the MRR and to lessen cutting device wear and surface harshness, and is generally influenced by current, pulse on time, and spark gap voltage, copper enjoys a clear benefit over graphite.

Additionally, MRR increases as the discharge current increases when copper electrodes are used, and the pulse can also reach the base EWR and ROC on time [13, 14]. The Ra value of the machined surface can provide a better surface finish on the EDM machined surface by using copper electrode, a lower discharge current, pulse on-time parameter setting, and expansion in discharge current and pulse on-time.

The creation of MoSi2-based composites can enhance crack growth, fracture toughness, and creep, according to Petrovic et al. [15]. $MoSi_2$-based composites use mechanisms such ductile phase toughening, continuous fiber reinforcement, transformation toughening, matrix micro cracking, and second phase whiskers and particles. Due to its high thermal conductivity, high melting point (2030 °C), low density (6.28 g/cm^2), and exceptional oxidation resistance/corrosion qualities, molybdenum disilicide (MoSi2) has been described by Gao et al. [16] as a suitable ceramic composite material for usage in high temperature parts and components. The fracture toughness and hardness of a composite made of silicon carbide and molybdenum disilicide were carefully examined by Zakeri et al. [17]. It was observed that SiC particles should have an ideal volume fraction for which the composite can attain extraordinary rupture toughness.

With an emphasis on the mechanisms of melting, vaporization, oxidation, breakdown, thermal spalling, electrostatic forces, and electromagnetic characteristics, MoSi2-SiC was examined in terms of material removal rate [18]. It can be concluded that additional components of the machining process need to be looked into because ceramic composites respond well to electrical discharge machining. Shabgard et al. talked about how applying a magnetic field to the EDM process might reduce the thickness of re-cast layers and increase plasma flushing effectiveness [19].

A mathematical model was created using the experimental value of SR, and it was 99 percent accurate in predicting the values [20]. Singh et al. RSM was used by Gourmand et al. [21] to examine the effects of EDM settings on Al-Mg_2Si MMCs with high MRR and low TWR. They found that the assessment error is less than 6.6%, proving that the models they projected are accurate. Using the RSM procedure, a minimum error has been reached for the performance measures [22].

According to Alduroobiet al. [23], the surface roughness increases with increases in peak current and pulse on time. They also found that the rate of electrode wear decreases with increases in pulse off time. According to Panda MR et al. [24], the presence of surface fissures and a molten ceramic pool on the machined surface suggested

thermal spalling during the machining process. According to Thangarajan Sivasankaran et al. [25], the smallest recast layer thickness and surface roughness were discovered at the process parameter condition gap current of 15 Amps, pulse on-time of 10 s, and pulse off-time of 6 s. According to Shahid Machno M et al. [26], the thickness of the recast layer increased when the discharge current was intensified. The worn surface was present around the cavity's perimeter and was caused by an increase in spark energy [27–30].

L. Selvarajan et al. investigates the spark erosion parameter to enhance drilled hole accuracy in intermetallic ceramic composites through testing and evaluation, contributing valuable insights to machining precision [31]. L. Selvarajan and K. Venkataramanan explores the surface morphology and drilled hole accuracy of Si3N4–TiN and $MoSi_2$–SiC conductive ceramic composites on EDMed surfaces, providing crucial information for improving the wear resistance of these materials [32]. L. Selvarajan et al. focuses on evaluating surface morphology in EDM processes for Si_3N_4-TiN, utilizing TLBO-MRA to optimize machining parameters [33]. L. Selvarajan and K. Venkataramanan delve into the evaluations of surface morphology in EDMed MoSi2-SiC intermetallic ceramic composite surfaces, contributing to the understanding of the material's machining characteristics [34]. L. Selvarajan et al. employs fuzzy logic optimization with regression analysis to enhance EDM machining parameters for Si_3N_4-TiN ceramic composites [35]. L. Selvarajan et al. provides an experimental analysis of holes made by electrical discharge machining on MoSi2-SiC composite, shedding light on the surface morphology of the machined components [36]. L. Selvarajan et al. conduct an experimental investigation on the surface morphology and recasting layer of Si_3N_4-TiN composites machined by die-sinking and rotary EDM [37]. L. Selvarajan et al. focuses on analyzing the geometrical errors of silicon nitride-titanium nitride during electric discharge machining using response surface methodology [38].

From the literature review, it seems that the effect of input process parameters such as polarity, pulse current, pulse on time, pulse off time, dielectric pressure, gap voltage, spark gap and servo speed on the machining output process parameters such as metal removal rate, electrode wear, wear ratio, and surface roughness and on the geometrical tolerance responses such as circularity, cylindricity, perpendicularity and radial overcut were discussed separately for the various materials. For the aim of machining ceramic composite, copper electrode is selected. After the drilling of the holes in the composite, the work piece is cut into cross—section using a wire EDM machine with molybdenum wire of 0.18 mm diameter since the Si_3N_4-TiN composite material cannot be cut by copper wire in WEDM machines, resulting to the usage of molybdenum wire. No researchers have been discussed with combination of machining output parameters and geometrical tolerance responses. Basically, the geometrical tolerances values are dependent on the machining output responses. Also, no work has been discussed on effect of servo speed on the geometrical tolerance of the machined surface. Hence, keeping this as a novelty, in this work we have discussed the effect of various input process parameters on the both machining output responses and geometrical tolerance responses.

2 Materials and Methodolgy

In this research, the work piece was made out of a 2 mm thick Si_3N_4-TiN Composites. The chromium zirconium copper rods used to construct the electrode started out 6 mm in diameter and 20 mm in length before being reduced to their final dimensions of 5 mm in diameter and 10 mm in length on a computer numerically controlled lathe. Chromium zirconium copper has a molecular formula of 1% chromium, 98.85% copper, and 0.15 percent zirconium. Adding zirconium to chromium copper improves the material's resistance to creep at high working temperatures and makes spot welding on coated or galvanised materials easier by reducing electrode sticking. Chromium zirconium copper has a density of 8.89 g/cm^2, among its other physical characteristics. An other material that may serve as a copper electrode is chrome zirconium copper [18]. The 18 holes were made using an OSCARMAX spark EDM (Model no. SD325-ZNC, place of origin: Thailand). The dielectric fluid feed was EDM oil. A high-precision electronic scale capable of reading increments as tiny as 0.001 g was used to weigh both the work piece and the electrodes. 18 holes, each 5 mm in diameter, are drilled for each EDMed experiment, and the work piece and electrodes are weighed both before and after machining. This investigation makes use of the Material Removal Mechanism approach, which entails melting and evaporation. The duration of the machining operation can be monitored with the help of a stop watch.

Relevant formulae have been implemented to arrive at process parameters including MRR, EWR and WR, etc., A surface tester machine can measure the roughness of a surface to within 5.5 µm of accuracy. Coordinate Measuring Instrument, GEOMET Model Accuracy: 4.5 mm Geometric tolerances such as roundness, cylindricity, and perpendicularity were calculated using GEOMET –Helmel's global CNC CMM software. To assess the circularity of a specimen, a CMM device probe is utilized to track eight peculiar features. After the hole was prepared for the CMM, the probe could move over its inner surface in 8 different locations. A line or surface that is perpendicular to the axis is one that meets it at a right angle. A coordinate measuring machine was used to assess the TRO, BRO, CIR, CYL, PER and RO. The mathematical modeling of each response

allows us to identify the causal link between process variables and outcome characteristics. The results show that the current has the biggest effect on MRR and EWR, whereas the pulse on time has the most effect on Overcut.

The Properties of Si_3N_4-TiN ceramic composite shown by Table 1 [32] and operating condition of the machine was shown by Table 2. The image of electrode was shown by Fig. 1 and Fig. 2 shows the machined work pieces after the EDM process. The $MoSi_2$-SiC ceramic composite's responses are listed in Table 3. The EDM used for this research work is shown in Fig. 3.

3 Results and Discussion

3.1 Pulse Current vs Output Responses

3.1.1 Material Removal Rate (MRR)

The EDM experiments on Si_3N_4-TiN ceramic composites revealed a direct relationship between pulse current and material removal rate. The analysis showed that as the pulse current increased, the material removal rate also increased simultaneously throughout the entire range of pulse currents.

As the pulse current increases, the energy delivered to the workpiece during each electrical discharge also increases. The higher discharge energy leads to more intense and efficient material removal, resulting in an increased material removal rate (Fig. 4).

The higher pulse current leads to a greater number of electrons flowing through the spark gap. This increased electron flow generates a higher-temperature plasma channel between the electrode and the workpiece. The elevated temperature and pressure cause localized melting and vaporization of the workpiece material, leading to more effective erosion and material removal.

Table 1 Properties of Si_3N_4-TiN ceramic composite

Property with unit	Si_3N_4-TiN
Young's Modulus of Elasticity (GPa)	341
Hardness (GPa)	90.5
Fracture Toughness (K^1C – MPa $m^{1/2}$)	5.7
Co efficient of Thermal Expansion (K^{-1})	5.6×10^{-6}
Thermal Conductivity (W/mK)	19.1
Electrical Resistivity (Ωm)	7.24×10^{-6}
Density (g/cc)	4.01
Poisson Ratio	0.31
Flextural Strength (MPa)	524 MPa
water absorption:	0.01—0.04%
open porosity	0.03%

The higher pulse current promotes the formation of a more intense and stable plasma channel between the electrode and the workpiece. This intensified plasma facilitates a higher level of material erosion and evaporation, results in increasing the material removal rate.

3.1.2 Electrode Wear Rate, Taper Angle, and Radial Overcut (ROC)

The experimental results suggest that as the pulse current increases, the electrode wear rate, taper angle, and ROC at the bottom initially increase due to increased discharge energy, electrode shape changes, thermal effects, and material removal efficiency. However, beyond a critical threshold, approximately 7 amperes, these parameters start to decrease due to improved material removal efficiency and stable machining conditions. On the other hand, the ROC at the top surface initially decreases due to optimal material removal, but beyond 7 amperes, it starts to increase due to excessive material removal and changes in the surface profile.

The initial increase in electrode wear rate, taper angle, and ROC at the bottom can be attributed to the higher discharge energy resulting in more significant material removal.

With higher pulse currents, the electrode experiences more frequent and intense electrical discharges, leading to increased wear and deformation. The changes in electrode shape can result in altered discharge dynamics, affecting the taper angle and ROC at the bottom surface.

Beyond a certain threshold, around 7 amperes, the increased pulse current may lead to improved material removal efficiency due to enhanced discharge energy and better flushing conditions. This results in reduced electrode wear rate, taper angle, and ROC at the top and bottom surface.

3.1.3 Wear Ratio

The experimental results suggest that as the pulse current increases, the wear ratio initially decreases due to optimal material removal and erosion. However, beyond a certain threshold, approximately 7 amperes, the wear ratio starts to increase drastically due to excessive material removal, thermal stress, changes in dielectric properties, material adherence, and alterations in the electrode shape.

As the pulse current increases, the energy delivered to the electrode and workpiece during each electrical discharge becomes higher. This leads to more intense material removal and erosion, which can result in reduced tool wear initially. The optimal material removal contributes to the decrease in the wear ratio.

Table 2 Experimental run order and machining time

Input Factor							
Polority	Current	Pulse on time	Pulse off time	Dielectric Pressure	Gap Voltage	Spark gap	Servo Speed
	amp	Ms	Ms	Kg/cm^2	v	mm	m/s
Positive	6	7	11	15	30	0.18	5
Positive	6	8	12	17	35	0.25	6
Positive	6	9	13	18	40	0.44	7
Positive	7	7	11	17	35	0.44	7
Positive	7	8	12	18	40	0.18	5
Positive	7	9	13	15	30	0.25	6
Positive	8	7	12	15	40	0.25	7
Positive	8	8	13	17	30	0.44	5
Positive	8	9	11	18	35	0.18	6
Negative	6	7	13	18	35	0.25	5
Negative	6	8	11	15	40	0.44	6
Negative	6	9	12	17	30	0.18	7
Negative	7	7	12	18	30	0.44	6
Negative	7	8	13	15	35	0.18	7
Negative	7	9	11	17	40	0.25	5
Negative	8	7	13	17	40	0.18	6
Negative	8	8	11	18	30	0.25	7
Negative	8	9	12	15	35	0.44	5

Workpiece Weight		Electrode Weight		Machining Time
Before Machining	After Machining	Before Machining	After Machining	Machining Time
gm	gm	gm	gm	Min
15.561	15.400	4.602	4.594	7.73
15.400	15.242	4.601	4.591	6.95
15.242	15.075	4.590	4.579	7.12
15.075	14.912	4.597	4.587	6.45
14.912	14.746	5.002	4.587	6.32
14.746	14.584	4.600	4.489	5.95
14.584	14.419	4.599	4.586	5.80
14.419	14.257	4.599	4.589	4.91
14.257	14.076	4.602	4.594	5.15
14.076	13.911	4.597	4.583	6.85
13.911	13.737	4.602	4.566	6.71
13.737	13.579	4.599	4.589	7.12
13.579	13.408	4.576	4.568	6.18
13.408	13.254	4.568	4.559	5.92
13.254	13.112	4.594	4.586	5.90
13.112	12.954	4.592	4.580	5.15
12.954	12.780	4.594	4.584	4.92
12.780	12.624	4.604	4.591	4.80

The higher pulse current can affect the dielectric properties of the EDM process. This includes changes in the dielectric breakdown strength, resistivity, and dielectric constant. Altered dielectric properties can influence discharge characteristics, spark formation, and material removal, ultimately impacting the wear ratio.

3.1.4 Circularity and Cylindricity

The experimental results suggest that as the pulse current increases, both circularity and cylindricity initially decrease slightly due to electrode wear and changes in machining dynamics. However, beyond a critical

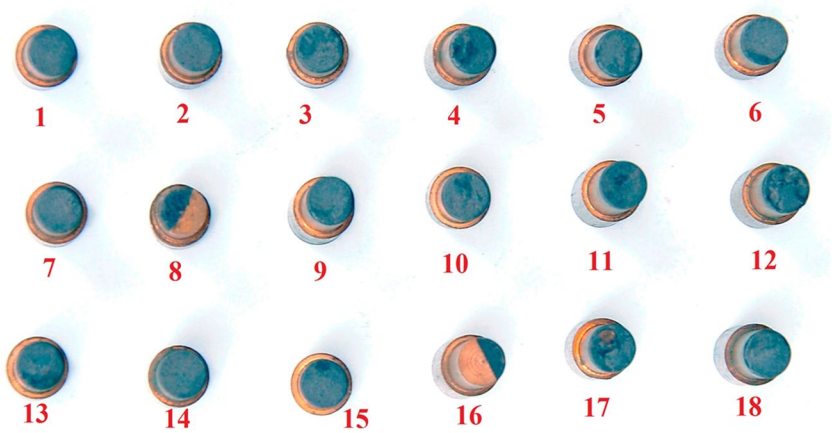

Fig. 1 Copper Multi-hole Electrodes by Laser Machining

threshold, approximately 7 amperes, both circularity and cylindricity decrease drastically due to excessive material removal, increased thermal effects, changes in dielectric properties, melt pool dynamics, and interaction with material properties.

The initial slight decrease in circularity and cylindricity can be attributed to the early stages of electrode wear and consequent changes in the machining dynamics, leading to alterations in the shape of the machined features.

The higher pulse current can affect the dielectric properties of the EDM process, such as dielectric breakdown strength, resistivity, and dielectric constant. These changes can influence spark formation, discharge characteristics, and material removal, impacting circularity and cylindricity.

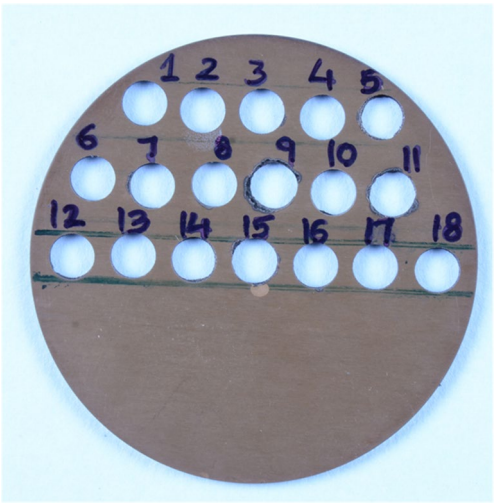

Fig. 2 Machined work piece by Copper Multi-hole Electrodes

3.1.5 Perpendicularity and Runout

The experimental results suggest that as the pulse current increases, both perpendicularity and run out increase simultaneously throughout the pulse current range. This behavior is mainly attributed to the increased discharge energy, electrode wear, thermal effects, material removal efficiency, changes in dielectric properties, and melt pool dynamics.

The higher discharge energy causes a more significant material removal process, which can result in increased tapering and run out on the machined surface.

The higher pulse current can affect the dielectric properties of the EDM process, such as dielectric breakdown strength, resistivity, and dielectric constant. These changes can influence spark formation, discharge characteristics, and material removal, impacting perpendicularity and run out.

3.1.6 Bottom and Top Diameter of the Drilled Hole

The experimental results suggest that as the pulse current increases, both the bottom diameter and top diameter of the drilled hole initially decrease due to increased discharge energy, electrode wear, thermal effects, and material removal efficiency. However, beyond a critical threshold, approximately 7 amperes, both dimensions start to increase due to improved material removal efficiency and stable machining conditions.

The higher discharge energy causes a more significant material removal process, resulting in the initial decrease in both the bottom diameter and top diameter of the drilled hole.

With higher pulse currents, the electrode experiences more frequent and intense electrical discharges, leading to increased wear and deformation. The changes in the electrode shape can result in altered discharge dynamics, affecting the drilling accuracy and the final dimensions of the drilled hole.

Table 3 Experimental results for responses after EDM

Response Parameter												
Material Removal Rate	Electrode Wear Rate	Wear Ratio	Circularity	Cylindricity	Perpendicularity	Ra	Top Diameter of drilled hole	Bottom Diameter of drilled hole	Run Out	ROC top	ROC bottom	Taper Angle
gm/min	gm/min		mm	mm	mm	µm	mm	mm	mm	mm	mm	deg
0.0208	0.001035	20.125	0.054	0.045	0.007	0.501	5.110	5.005	0.039	0.055	0.002	0.759
0.0227	0.001439	15.8	0.059	0.050	0.011	0.346	5.108	5.043	0.078	0.054	0.022	0.458
0.0235	0.001545	15.18182	0.062	0.046	0.036	0.555	5.111	5.017	0.036	0.055	0.009	0.687
0.0253	0.00155	16.3	0.053	0.044	0.042	0.229	5.107	5.027	0.370	0.054	0.014	0.572
0.0263	0.065665	0.4	0.057	0.036	0.051	0.317	5.124	4.572	0.378	0.062	-0.214	3.947
0.0272	0.018655	1.459459	0.070	0.034	0.016	0.335	5.133	4.948	0.097	0.067	-0.026	1.317
0.0284	0.002241	12.69231	0.097	0.042	0.026	0.269	5.087	4.975	0.131	0.043	-0.013	0.802
0.0330	0.002037	16.2	0.067	0.035	0.051	0.963	5.098	5.012	0.329	0.049	0.006	0.630
0.0351	0.001553	22.625	0.154	0.151	0.195	0.444	5.562	5.351	0.839	0.281	0.176	1.489
0.0241	0.002044	11.78571	0.058	0.043	0.016	0.117	5.186	5.042	0.103	0.093	0.021	1.031
0.0259	0.005365	4.833333	0.118	0.107	0.023	0.461	5.221	5.043	0.184	0.111	0.022	1.260
0.0222	0.001404	15.8	0.039	0.043	0.007	0.598	5.126	4.946	0.048	0.063	-0.027	1.317
0.0277	0.001294	21.375	0.040	0.034	0.020	0.270	5.091	4.992	0.123	0.046	-0.004	0.687
0.0260	0.00152	17.11111	0.050	0.046	0.008	1.618	5.099	4.866	0.067	0.050	-0.067	1.661
0.0241	0.001356	17.75	0.114	0.129	0.220	0.271	5.173	4.998	0.924	0.087	-0.001	1.260
0.0307	0.00233	13.16667	0.042	0.046	0.107	0.401	5.099	4.984	0.671	0.050	-0.008	0.802
0.0354	0.002033	17.4	0.054	0.059	0.026	0.602	5.119	5.013	0.208	0.059	0.006	0.744
0.0325	0.002708	12	0.063	0.056	0.046	0.310	5.139	4.909	0.356	0.070	-0.046	1.661

Fig. 3 Electrical Discharge Machine

3.1.7 Surface Roughness

The experimental results suggest that as the pulse current increases, the surface roughness of the machined Si_3N_4-TiN ceramic composites increases simultaneously throughout the pulse current range. This behavior is mainly attributed to the increased discharge energy, material removal efficiency, melting and resolidification effects, changes in dielectric properties, and thermal damage to the workpiece surface. The results indicate that increasing the pulse current can lead to higher surface roughness due to the more aggressive material removal and thermal effects.

The intense heat generated by higher pulse currents can lead to localized melting of the workpiece material. Subsequently, the molten material may resolidify in a slightly deformed state, leading to irregularities on the machined surface and contributing to surface roughness. The rapid heating and cooling cycles during EDM can cause localized thermal damage to the workpiece surface, leading to the formation of micro-cracks, pits, and other defects, which can increase the surface roughness.

3.2 Dielectric Pressure vs Output Responses

3.2.1 Material Removal Rate, Electrode Wear Rate, ROC Top and Top Diameter of the Drilled Hole

The Electrical Discharge Machining (EDM) of Si_3N_4-TiN ceramic composites, the dielectric pressure plays a crucial role in the material removal process and the resulting characteristics of the drilled hole (Fig. 5). The observed changes in material removal rate, electrode wear rate, rate of change of top radius of curvature (ROC top), and top diameter of the drilled hole can be explained by the following mechanisms:

At lower dielectric pressure, the spark energy may not be sufficient to facilitate efficient material removal. This results in a relatively slower material removal rate and a lesser wear of the electrode. The low dielectric pressure leads to a less forceful flushing action, which might cause the electrode to remain in closer proximity to the workpiece surface, resulting in a smaller ROC top and a reduced top-hole diameter.

Increasing the dielectric pressure significantly improves the flushing action during EDM, leading to better spark distribution and improved material removal rate. However, the higher dielectric pressure can also lead to an increase in the

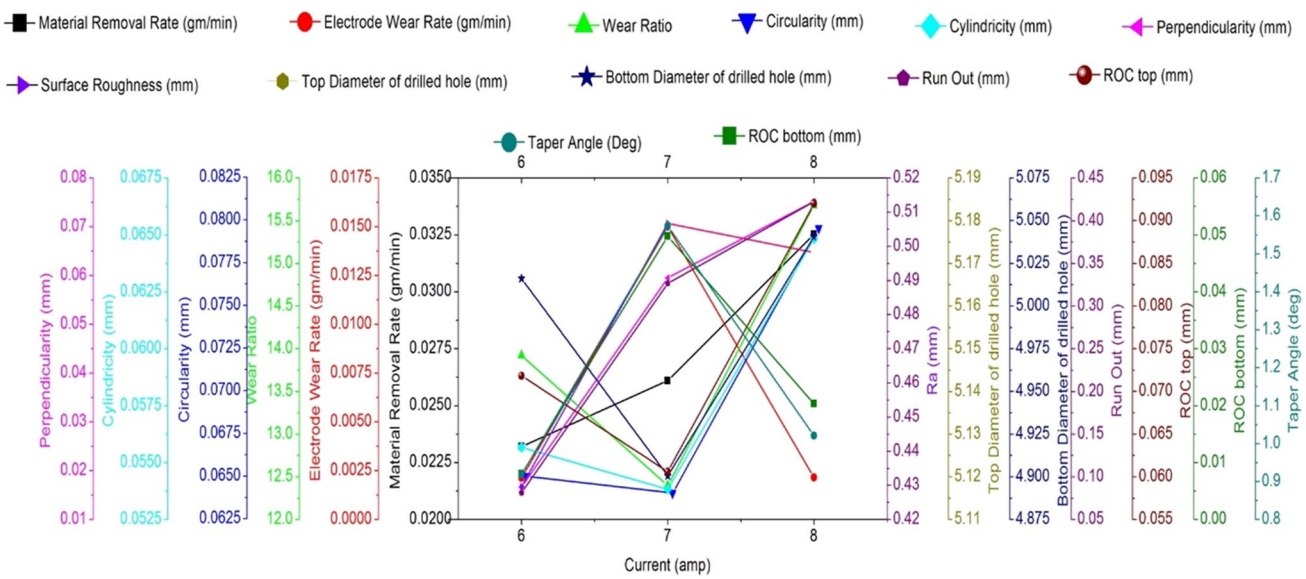

Fig. 4 Current Vs Output Parameters

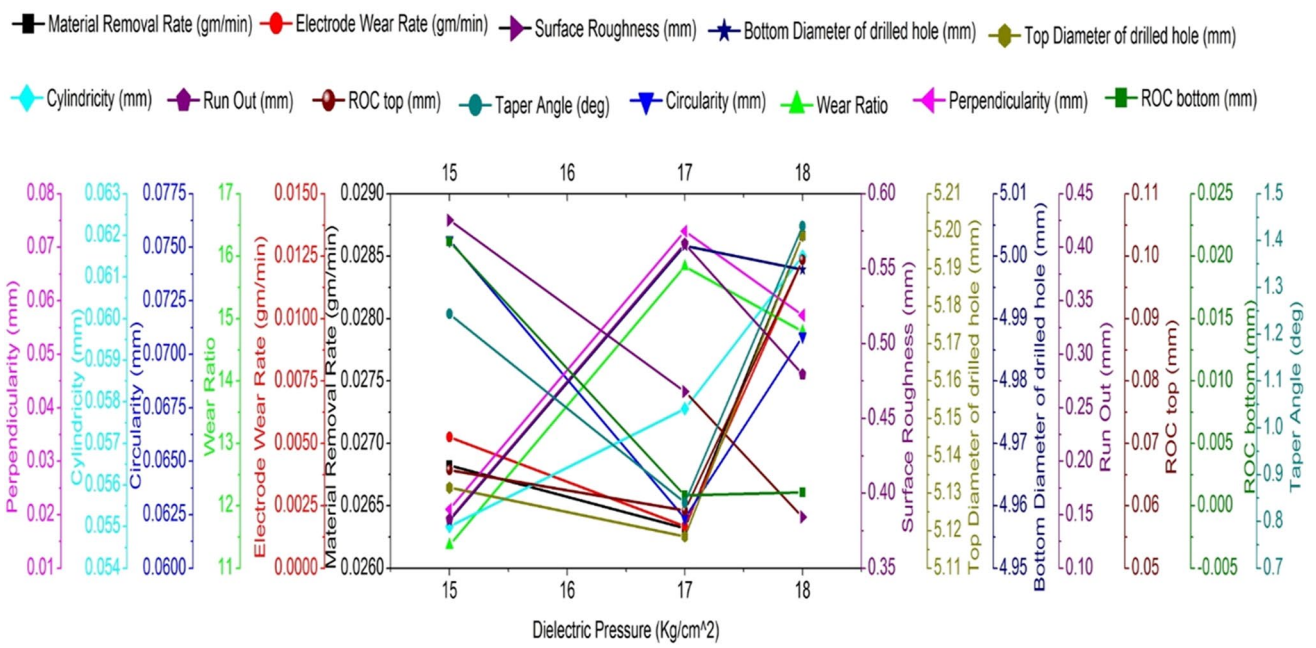

Fig. 5 Dielectric Pressure Vs Output Parameters

number of sparks and their intensity, causing a more aggressive wear of the electrode and resulting in a higher electrode wear rate. The enhanced flushing action and higher spark intensity can also lead to increased energy concentration at the workpiece surface, resulting in a more significant melting and vaporization of the material. Consequently, this leads to an increase in the ROC top and a larger top hole diameter.

The experimental results revealed that when the dielectric pressure was maintained below 17 kg/cm^2, the material removal rate, electrode wear rate, ROC top, and top diameter of the drilled hole were observed to decrease slightly. This behavior can be attributed to the limited energy provided by the sparks at lower dielectric pressures, leading to less efficient material removal and reduced wear of the electrode. The smaller ROC top and hole diameter can be explained by the weaker flushing action at lower pressures, which keeps the electrode closer to the workpiece surface during the machining process. Conversely, when the dielectric pressure was increased to 17 kg/cm^2 and beyond, there was a drastic increase in the material removal rate, electrode wear rate, ROC top, and top diameter of the drilled hole. This phenomenon can be understood by the combined effect of improved flushing action and higher spark intensity. The enhanced flushing action helps in better spark distribution and material removal, leading to a higher material removal rate. However, the increased spark intensity causes more aggressive wear of the electrode, leading to a higher electrode wear rate.

3.2.2 Wear Ratio, Runout, Perpendicularity, and Top Diameter of the Drilled Hole

The experimental results demonstrate that with increasing dielectric pressure up to 17 kg/cm^2, the wear ratio, runout, perpendicularity, and top diameter of the drilled hole increase drastically. This behavior can be attributed to the combined effects of improved flushing action and intensified sparking. The stronger flushing action promotes better spark distribution, but the higher spark intensity leads to more aggressive wear of the electrode, deviations in perpendicularity, and increased top diameter.

When the dielectric pressure is increased up to 17 kg/cm^2, the enhanced flushing action promotes better spark distribution and material removal. However, it also results in more aggressive sparking, leading to a higher wear ratio. The increased dielectric pressure can intensify the sparks and concentrate the energy on the electrode, causing higher localized wear and erosion, thereby increasing the wear ratio. Beyond 17 kg/cm^2, the dielectric pressure may reach a level where the excessive flushing action and spark intensity lead to rapid electrode wear and erosion.

The increased dielectric pressure causes stronger flushing action, which can lead to increased electrode movement or vibrations. This excessive movement or vibrations may lead to higher runout, indicating deviations from the desired axis of rotation or concentricity of the electrode during the machining process. At very high dielectric pressures, the

strong flushing action can help stabilize the EDM process. This improved stability may result in reduced electrode movement and vibrations, leading to a decrease in runout.

As the dielectric pressure is raised, the flushing action becomes more forceful, causing increased material removal. However, due to the aggressive sparking at higher pressures, the EDM process may become less stable and less controlled, leading to deviations in the perpendicularity of the drilled hole with respect to the workpiece surface. As the dielectric pressure increases beyond 17 kg/cm^2, the EDM process may become more stable and controlled.

The improved flushing action at higher dielectric pressures contributes to more efficient material removal, which results in an increase in the top hole diameter. Additionally, the higher sparking intensity can lead to broader melting and vaporization zones at the top surface of the hole, further contributing to the increased top diameter. At very high dielectric pressures, the increased spark intensity and energy concentration may lead to more precise and localized material removal.

3.2.3 Taper Angle and Circularity

The experimental results demonstrate that as the dielectric pressure is increased up to 17 kg/cm^2, the taper angle and circularity of the drilled hole drastically decrease. This behavior can be attributed to the combined effect of improved flushing action, better spark distribution, and reduced spark intensity at lower dielectric pressures.

As the dielectric pressure increases up to 17 kg/cm^2, the flushing action becomes more forceful and efficient. The improved flushing action helps in better spark distribution, leading to more uniform and distributed material removal along the electrode's axial direction. This results in a reduction of the taper angle, indicating less deviation from the desired perpendicularity of the drilled hole, and an improvement in circularity.

At lower dielectric pressures, the spark intensity may not be as high due to limited energy provided by the sparks. The lower spark intensity results in a softer and less aggressive material removal process, which can contribute to a smoother and more uniform hole profile, leading to decreased taper angle and improved circularity.

Beyond 17 kg/cm^2, the dielectric pressure may reach a level where the spark intensity becomes too high and concentrated. The intensified sparks can cause more aggressive material removal and electrode erosion, leading to a rougher and less uniform hole profile. This can result in an increase in taper angle, indicating a larger deviation from perpendicularity, and a decrease in circularity, indicating a less concentric hole.

At very high dielectric pressures, the increased sparking intensity can lead to rapid electrode wear and erosion. As the electrode wears and changes shape, its effectiveness as a tool diminishes, causing variations in the EDM process and negatively impacting hole quality. The irregular shape of the electrode can lead to deviations in the machined hole, contributing to increased taper angle and reduced circularity.

3.2.4 ROC Bottom

The experimental results demonstrate that as the dielectric pressure increases up to 17 kg/cm^2, the rate of change of the bottom radius of curvature (ROC bottom) drastically decreases. This behavior can be attributed to the combined effect of enhanced material removal and aggressive sparking at higher dielectric pressures. The increased flushing action and spark intensity result in a faster removal of material from the workpiece surface, leading to a significant reduction in the bottom radius of curvature.

As the dielectric pressure increases up to 17 kg/cm^2, the flushing action becomes more forceful, leading to improved spark distribution and better material removal. The increased flushing action aids in efficiently removing material from the workpiece surface, leading to a faster decrease in the bottom radius of curvature (ROC bottom).

3.2.5 Surface Roughness

The experimental results demonstrate that as the dielectric pressure is increased, the surface roughness of Si_3N_4-TiN ceramic composites decreases gradually. This behavior can be attributed to the combined effects of enhanced flushing action, improved spark distribution, reduced electrode wear, and suppression of melting and vaporization.

As the dielectric pressure increases, the flushing action becomes more forceful and efficient. The improved flushing action helps in the efficient removal of debris, eroded material, and dielectric fluid from the machining zone. As a result, the recast layer (re-deposited material on the machined surface) is minimized, leading to a smoother surface finish and reduced surface roughness.

Higher dielectric pressure promotes better spark distribution, ensuring more uniform material removal. The improved spark distribution helps in reducing localized melting and vaporization, which can lead to uneven surface roughness.

3.2.6 Cylindricity

The experimental results demonstrate that as the dielectric pressure increases, the cylindricity of the drilled hole in Si_3N_4-TiN ceramic composites increases gradually. This behavior can be attributed to the combined effects of enhanced flushing action, improved spark distribution, reduced electrode wear and suppression of melting and vaporization.

As the dielectric pressure increases, the flushing action becomes more forceful and efficient. The improved flushing action helps in the better removal of debris and eroded material

from the machining zone, leading to a cleaner and more uniform hole profile. The increased dielectric pressure also promotes better spark distribution, ensuring more uniform material removal along the entire circumference of the drilled hole.

3.3 Gap Voltage vs Output Responses

3.3.1 Circularity, Cylindricity, Runout, Perpendicularity, ROC Bottom and Taper Angle

The experimental results demonstrate that as the gap voltage is increased in the EDM of Si_3N_4-TiN ceramic composites, the Circularity, Cylindricity, Runout, Perpendicularity, ROC Bottom, and Taper Angle increase gradually. These observations can be attributed to the combined effects of increased spark energy, intensified sparking, electrode wear, and overflushing effects (Fig. 6).

Higher gap voltage promotes intensified sparking, with more sparks occurring per unit time. The intensified sparking causes more material to be melted, vaporized, and eroded, leading to increased recast layer and material redeposition. This can cause irregularities on the machined surface, contributing to variations in Circularity, Cylindricity, Runout, Perpendicularity, ROC Bottom, and Taper Angle.

3.3.2 Wear ratio, ROC Top, Top Diameter of Drilled Hole and Bottom Diameter of Drilled Hole

The experimental results demonstrate that as the gap voltage increases, the ROC_{Top} and Top diameter of the drilled hole drastically increase, while the Wear ratio and Bottom diameter of the drilled hole increase. This behaviour can be attributed to the combined effects of increased spark energy, intensified sparking, and electrode wear.

As the gap voltage increases, the potential difference between the electrode and workpiece also increases. This results in higher spark energy during the electrical discharges. The intensified sparking, caused by higher gap voltage, leads to more energetic sparks and greater material removal rates. The increased spark energy and intensified sparking cause more extensive melting, vaporization, and erosion at the workpiece surface, leading to larger ROC Top and an increased Top diameter of the drilled hole.

With higher spark energy and intensified sparking due to increased gap voltage, the electrode undergoes more significant wear and erosion. The higher wear rate of the electrode results in increased electrode material being deposited on the machined surface (recast layer) and an increase in the Bottom diameter of the drilled hole.

3.3.3 Material Removal Rate and Surface Roughness

The experimental results demonstrate that as the gap voltage increases, the Material Removal rate and Surface roughness in the EDM of Si_3N_4-TiN ceramic composites slightly decrease. This behavior can be attributed to the combined effects of increased spark energy, intensified sparking, and enhanced melting and vaporization at the workpiece surface.

As the gap voltage increases, the potential difference between the electrode and workpiece also increases. This results in higher spark energy during the electrical discharges. The intensified sparking, caused by higher gap voltage, leads to more energetic sparks and greater material removal rates. However, the

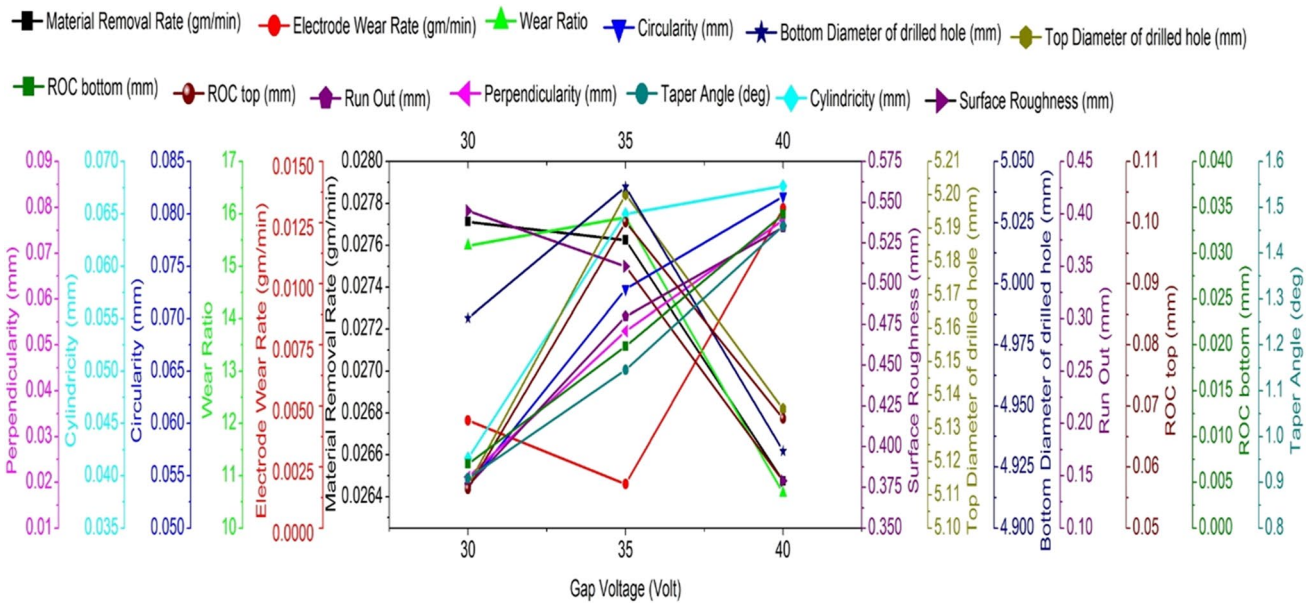

Fig. 6 Gap Voltage Vs Output Parameters

increased spark energy can also lead to enhanced melting and vaporization at the workpiece surface, resulting in a smoother surface finish and slightly decreased surface roughness.

Beyond a certain threshold, typically 35 V, the gap voltage may become excessively high, leading to overflushing effects. Overflushing can cause excessive removal of material, leading to a decrease in the material removal rate. Additionally, at very high gap voltages, the EDM process may become less stable, leading to a more erratic and less controlled material removal process, resulting in a drastic decrease in material removal rate and surface roughness.

3.3.4 Electrode Wear Rate

The experimental results demonstrate that as the gap voltage increases, the electrode wear rate in the EDM of Si_3N_4-TiN ceramic composites decreases. This behavior can be attributed to the combined effects of increased spark energy, intensified sparking, and reduced material deposition on the electrode.

The higher spark energy and intensified sparking due to increased gap voltage result in more efficient material removal from the workpiece, leading to less material being deposited on the electrode surface, thus reducing the electrode wear rate.

However, beyond a certain threshold, typically 35 V, the gap voltage becomes excessively high, leading to aggressive erosion and wear of the electrode surface. The higher gap voltage causes intensified sparking and aggressive material removal, resulting in more significant melting, vaporization, and erosion of the electrode material, leading to a drastic increase in the rate of electrode wear.

3.4 Pulse on time Vs Output Responses

3.4.1 Material Removal Rate, Electrode Wear Rate, Surface Roughness, Taper Angle and ROC Bottom

The experimental results demonstrate that as the pulse on time increases from 7 to 8 microseconds, the Material Removal Rate, Electrode Wear Rate, Surface Roughness, Taper Angle, and ROC Bottom increase drastically. This behaviour can be attributed to the increased energy input, enhanced melting and vaporization, thicker recast layer, and aggressive material removal at the workpiece surface (Fig. 7).

As the pulse on time increases, the duration of each electrical discharge between the electrode and workpiece also increases. This leads to an increased energy input during each discharge event. The increased energy input results in more aggressive material removal from the workpiece, leading to a higher Material Removal Rate.

With longer pulse on time, there is more time for the spark energy to heat and melt the workpiece material. The extended pulse duration promotes deeper melting and vaporization at the workpiece surface, leading to a higher Electrode Wear Rate due to increased material loss from the electrode.

The increased energy input and extended pulse duration also contribute to more aggressive material removal, leading to a higher Taper Angle and larger ROC Bottom. The Taper Angle increases due to enhanced material removal at the upper portion of the drilled hole, while the larger ROC Bottom indicates a more pronounced curvature at the bottom of the hole.

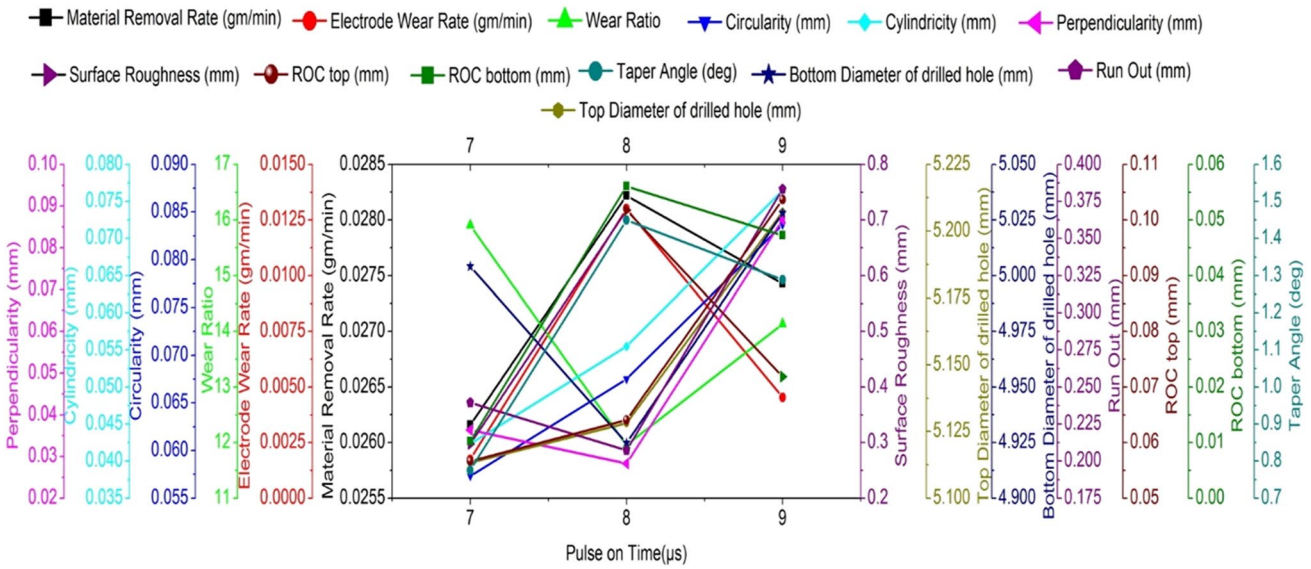

Fig. 7 Pulse on Time Vs Output Parameters

Beyond a certain threshold, typically beyond 8 microseconds, the extended pulse on time may cause over burning of the work piece surface. Over burning refers to excessive and uncontrolled material removal, which can lead to decreased Material Removal Rate and Taper Angle due to over-aggressive material removal. However, at very high pulse on times, the material removal may become more stable, and the electrode wear rate can decrease as the spark energy becomes more evenly distributed.

3.4.2 Wear Ratio, Bottom Diameter of Drilled Hole, Runout and Perpendicularity

The experimental results demonstrate that as the pulse on time increases from 7 to 8 microseconds, the Wear Ratio and Bottom diameter of the drilled hole decrease drastically. This behavior can be attributed to the improved material removal efficiency and smoother, more controlled spark discharge during the longer pulse on time.

As the pulse on time increases, the duration of each electrical discharge between the electrode and workpiece also increases. This results in a longer period of material removal during each discharge event. The increased pulse on time leads to a more efficient and consistent material removal process, resulting in a decrease in the Wear Ratio and a reduction in the Bottom diameter of the drilled hole.

Longer pulse on time allows for a smoother and more controlled spark discharge between the electrode and workpiece. This smoother discharge can contribute to a more uniform and precise material removal process, leading to a decrease in Runout and Perpendicularity.

At very long pulse on times, the EDM process may become less stable due to overburning and other factors. The reduced stability can lead to less uniform and less controlled material removal, resulting in an increase in the Wear Ratio and decreased dimensional accuracy, reflected in higher Runout and Perpendicularity.

3.4.3 Top Diameter of Drilled Hole, ROC Top, Circularity and Cylindricity

The experimental results demonstrate that as the pulse on time increases from 6 to 8 microseconds, the Top diameter of the drilled hole, ROC Top, Circularity, and Cylindricity gradually increase. This behavior can be attributed to the combined effects of extended material removal duration, enhanced melting and material redistribution, and improved hole shape conformity during the longer pulse on time.

As the pulse on time increases, the duration of each electrical discharge event between the electrode and workpiece also increases. This results in a longer period of material removal during each discharge. The increased pulse on time allows more material to be eroded from the workpiece, leading to a gradual increase in the Top diameter of the drilled hole.

3.5 Pulse off time Vs Output Responses

3.5.1 Material Removal Rate, Bottom Diameter of Drilled Hole, Top Diameter of Drilled Hole, Surface Roughness, Perpendicularity, Run out and ROC Top

The experimental results demonstrate that as the pulse-off time increases from 11 to 12 microseconds, the Material Removal Rate, Bottom Diameter of Drilled Hole, Top Diameter of Drilled Hole, Perpendicularity, Runout, and ROC Top drastically decrease, while the Surface Roughness slightly decreases. This behavior can be attributed to reduced material removal efficiency, increased cooling and solidification, reduced sparking and material redistribution, and the formation of a smoother surface during the longer pulse-off time (Fig. 8).

As the pulse-off time increases, the duration between successive electrical discharge events (pulses) also increases. Longer pulse-off time leads to a longer interval between spark discharges, resulting in reduced material removal efficiency. The decreased material removal efficiency contributes to a drastic decrease in Material Removal Rate.

Longer pulse-off time allows for more cooling and solidification of the molten material around the drilled hole during the interval between pulses. The increased cooling and solidification restrict the material's flow and prevent it from being effectively removed, leading to a reduction in the Bottom Diameter of the Drilled Hole and Top Diameter of the Drilled Hole.

With longer pulse-off time, the energy input during the spark discharge is reduced due to a longer interval between pulses. The decreased energy input results in less melting and material redistribution during each spark discharge, leading to a decrease in Perpendicularity, Runout, and ROC Top.

The increased cooling and solidification during the longer pulse-off time contribute to the formation of a smoother surface. The smoother surface results in a slightly reduced Surface Roughness.

Beyond a certain threshold, typically beyond 12 microseconds, the increased pulse-off time may allow for better flushing of debris and eroded material from the machining zone. Improved flushing can result in more efficient material removal during each spark discharge, leading to a drastic increase in Material Removal Rate.

3.5.2 Wear Ratio, Cylindricity and Circularity

The experimental results demonstrate that as the pulse-off time increases from 11 to 12 microseconds, the Wear Ratio,

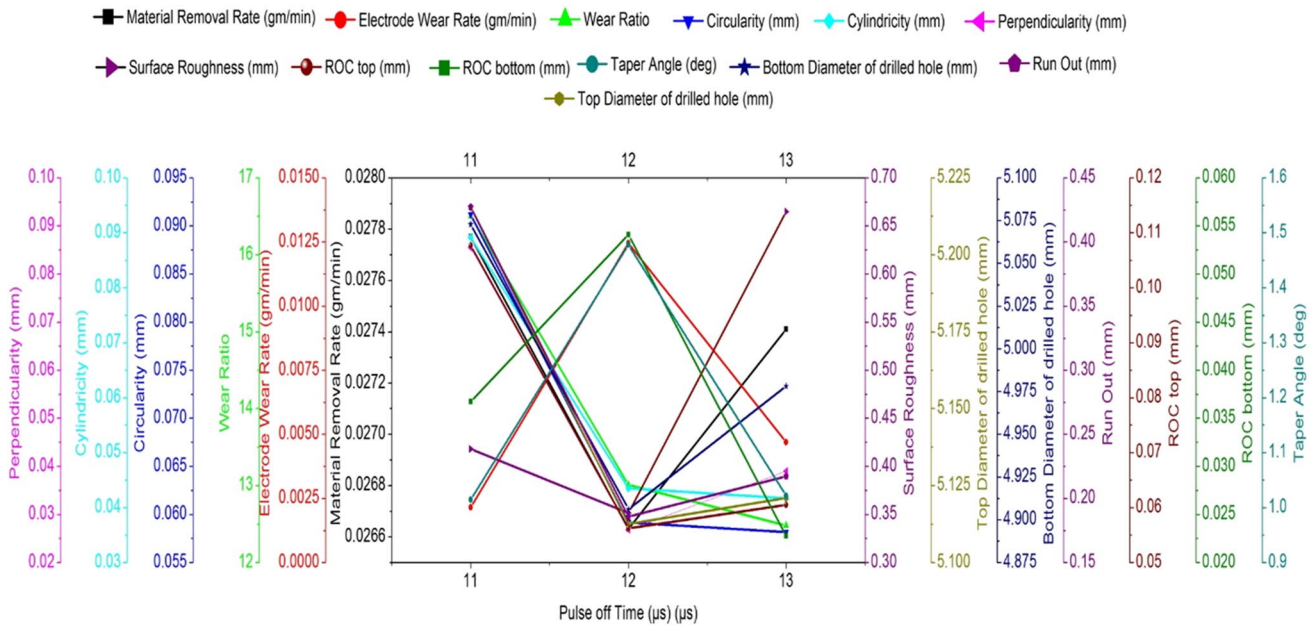

Fig. 8 Pulse off Time Vs Output Parameters

Cylindricity, and Circularity drastically decrease. This behavior can be attributed to the reduced material removal efficiency and the increased solidification and smoother surface formation during the longer pulse-off time.

As the pulse-off time increases, the duration between successive electrical discharge events (pulses) also increases. Longer pulse-off time leads to a longer interval between spark discharges, resulting in reduced material removal efficiency. The decreased material removal efficiency contributes to a drastic decrease in the Wear Ratio.

Beyond a certain threshold, typically beyond 12 microseconds, the increased pulse-off time allows for better flushing of debris and eroded material from the machining zone. This improved flushing action can lead to more efficient material removal during each spark discharge, resulting in a slight decrease in the Wear Ratio.

The increased material removal efficiency and improved flushing action at longer pulse-off times can contribute to better dimensional control of the machined hole. As a result, the Cylindricity and Circularity may slightly decrease due to better stability and control in the material removal process.

3.5.3 Electrode Wear Rate, ROC Bottom and Taper angle

The experimental results demonstrate that as the pulse-off time increases from 11 to 12 microseconds, the Electrode Wear Rate, ROC Bottom, and Taper Angle increase drastically. This behavior can be attributed to reduced cooling and erosion stabilization, the accumulation of molten material on the electrode surface, and increased material removal efficiency during the longer pulse-off time.

As the pulse-off time increases, the duration between successive electrical discharge events (pulses) also increases. Longer pulse-off time results in a longer interval between spark discharges, leading to reduced cooling of the electrode between pulses. The reduced cooling inhibits the stabilization of the electrode surface, leading to increased electrode wear due to more aggressive erosion.

Beyond a certain threshold, typically beyond 12 microseconds, the increased pulse-off time allows for better cooling and stabilization of the electrode surface. The improved cooling and stabilization contribute to a reduction in the electrode wear rate as the electrode surface is less susceptible to aggressive erosion.

At very long pulse-off times, the improved cooling and stabilization can also lead to reduced material removal efficiency during each spark discharge. The reduced material removal efficiency results in a decrease in the ROC Bottom and Taper Angle due to less material loss from the workpiece.

3.6 Spark Gap Vs Output Responses

3.6.1 Cylindricity and Perpendicularity

The experimental results demonstrate that as the spark gap increases from 0.18 mm to 0.44 mm, the Circularity and Perpendicularity reduce gradually. This behavior can be attributed to the increased spark energy dissipation,

diffusion, spark erosion, reduced spatial resolution, and increased electrode wear at larger spark gaps (Fig. 9).

The increased spark gap leads to higher electrical resistance and weaker sparks, which affects the precision of material removal and reduces Circularity and Perpendicularity. As the spark gap increases, the distance between the electrode and workpiece also increases. A larger spark gap leads to higher electrical resistance, resulting in increased spark energy dissipation during the discharge process. The increased spark energy dissipation causes a weaker and less energetic spark, affecting the precision of material removal.

3.6.2 Run out, Electrode Wear Rate, ROC Bottom, ROC TOP and Taper Angle

The experimental results demonstrate that as the spark gap increases from 0.18 mm to 0.25 mm, the Runout, Electrode Wear Rate, ROC Bottom, ROC Top, and Taper Angle drastically reduce. This behavior can be attributed to the increased spark energy concentration, improved spark discharge control, and reduced electrode wear rate at larger spark gaps.

Beyond a certain threshold, typically beyond 0.25 mm, the spark gap becomes less critical in affecting the EDM process parameters. As the spark gap further increases, the EDM system may tolerate slight variations without significant impacts on the machining precision.

3.6.3 Bottom Diameter of the Drilled Hole and Circularity

The experimental results demonstrate that as the spark gap increases from 0.18 mm to 0.25 mm, the Bottom Diameter of the drilled hole and Circularity increase drastically. This behavior can be attributed to the increased spark energy concentration, improved material removal efficiency, and enhanced EDM stability at larger spark gaps.

As the spark gap increases, the distance between the electrode and workpiece also increases. With a larger spark gap, the electrical discharge events become more concentrated in a smaller area on the workpiece. The increased spark energy concentration results in more efficient and localized material removal during each spark discharge.

Larger spark gaps allow for higher energy discharges that result in more efficient and controlled material removal from the workpiece. The increased material removal efficiency contributes to a larger Bottom Diameter of the drilled hole and improved Circularity.

Larger spark gaps provide a more stable and controlled spark discharge environment, reducing the chances of erratic or uneven material removal. The increased stability enhances the dimensional accuracy and improves Circularity.

3.6.4 Material Removal Rate

The experimental results demonstrate that as the spark gap increases from 0.18 mm to 0.44 mm, the Material Removal Rate increases gradually. This behavior can be attributed to the increased spark energy concentration, enhanced material removal efficiency, increased heat generation, and improved debris flushing at larger spark gaps. The increased spark energy concentration results in higher energy input to the workpiece during each spark discharge, leading to more efficient material removal. Additionally, the enhanced material removal efficiency at larger spark gaps is facilitated by the increased heat generation, which softens the material and makes it more susceptible to removal during the spark

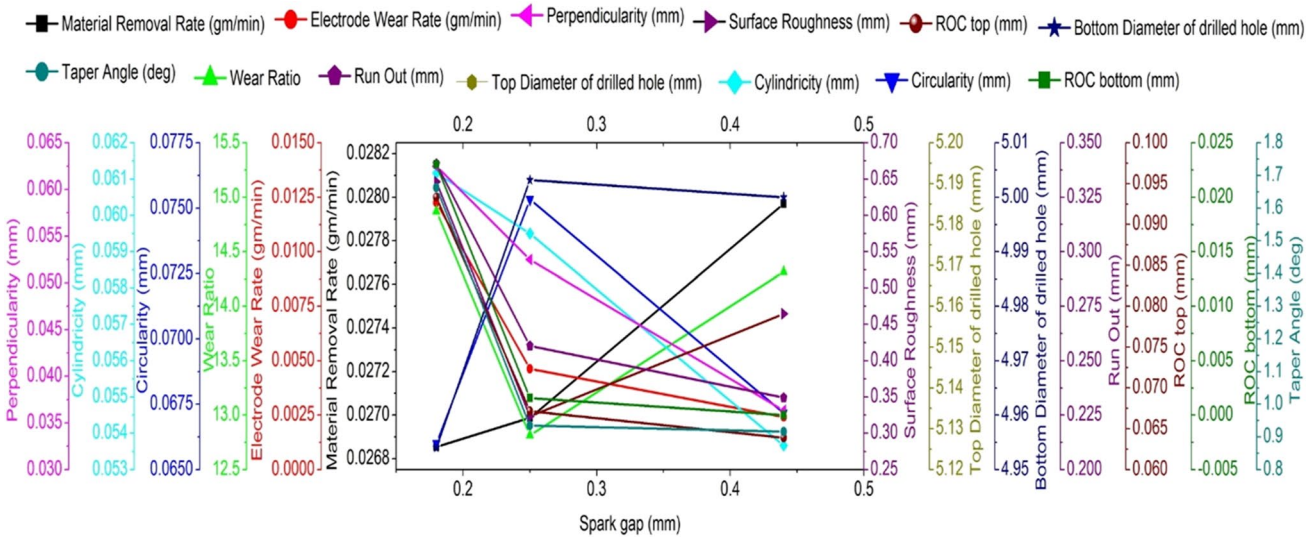

Fig. 9 Spark gap Vs Output Parameters

discharge process. Moreover, the improved debris flushing at larger spark gaps prevents re-deposition of eroded material, allowing for continuous and efficient material removal, further contributing to the gradual increase in Material Removal Rate.

3.6.5 Wear Ratio

The experimental results demonstrate that as the spark gap increases from 0.18 mm to 0.25 mm, the Wear Ratio decreases drastically. This behavior can be attributed to the increased spark energy concentration, enhanced material removal efficiency, and reduced electrode wear rate at larger spark gaps.

As the spark gap increases, the distance between the electrode and workpiece also increases. With a larger spark gap, the electrical discharge events become more concentrated in a smaller area on the workpiece. The increased spark energy concentration results in higher energy input to the workpiece during each spark discharge.

Beyond a certain threshold, typically beyond 0.25 mm spark gap, the spark energy starts to disperse over a wider area on the workpiece. The reduced spark energy concentration leads to less efficient and more diffused material removal during each spark discharge.

3.7 Servo Speed Vs Output Responses

3.7.1 Material Removal Rate

The material removal rate was found to increase with an increase in servo speed up to 6 m/s, after which it started to decrease (Fig. 10).

At lower servo speeds (5 m/s), the EDM process exhibited a relatively low energy discharge, resulting a material removal rate of 0.02655 gm/min. As the servo speed was increased to 6 m/s, the discharge energy became more intense, leading to higher material removal rates. This phenomenon can be attributed to the increased frequency of electrical discharges, which resulted in a greater number of removal events on the workpiece surface.

The optimal material removal rate was achieved at a servo speed of 6 m/s. Beyond this speed, the material removal rate started to decrease. This decrease can be attributed to several factors. First, at higher servo speeds, the energy of the electrical discharges might have exceeded the threshold for efficient material removal, leading to the formation of larger craters and debris, which could reduce the overall material removal efficiency.

3.7.2 Electrode Wear Rate

The EDM experiments on Si_3N_4-TiN ceramic composites demonstrated a remarkable reduction in electrode wear rate with increasing servo speed. The data obtained from the experiments revealed that as the servo speed increased, the electrode wear rate consistently decreased.

As the servo speed increases, the movement of the electrode becomes faster and more dynamic. This enhanced motion facilitates better flushing of dielectric fluid and electrode debris from the spark gap region. Effective flushing helps in removing the eroded particles and debris from the machining area, reducing the chances of re-deposition of material on the electrode surface. Consequently, the electrode experiences reduced contact with recast material, leading to a decrease in wear.

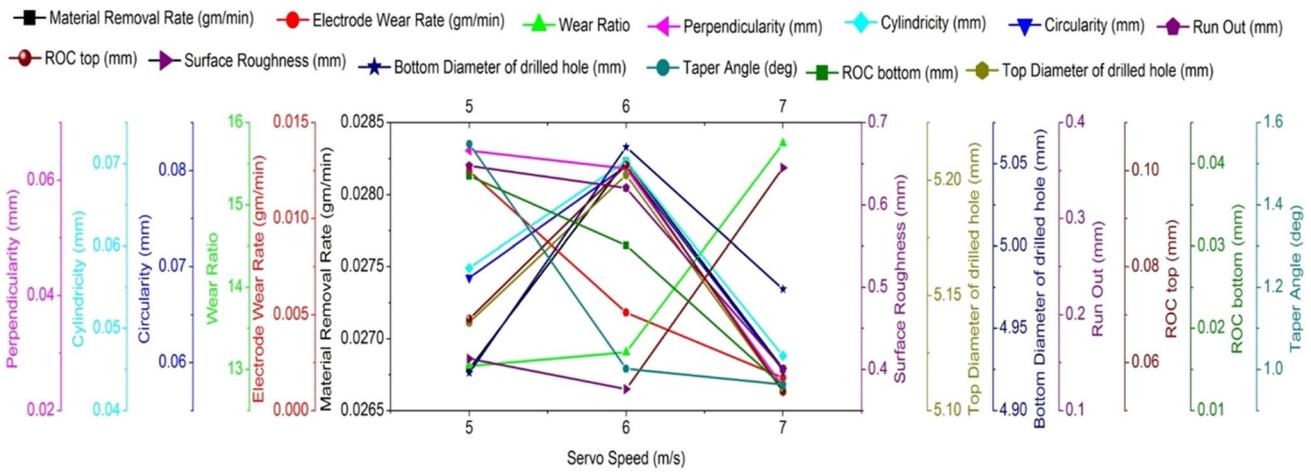

Fig. 10 Servo Speed Vs Output Parameters

3.7.3 Wear Ratio

The EDM experiments on Si_3N_4-TiN ceramic composites revealed a consistent increase in the wear ratio with increasing servo speed. The data obtained from the experiments clearly demonstrated that as the servo speed increased, the wear ratio also increased. The mechanism analysis provides insights into why this phenomenon occurs. The intensified thermal effects at higher servo speeds lead to more severe material erosion and wear on both the workpiece and the electrode. This, in turn, contributes to the higher wear ratio observed in the experiments.

As the servo speed increases, the frequency of electrical discharges also increases. Moreover, the higher material removal rate at elevated servo speeds is a double-edged sword. While it results in increased machining efficiency, it also leads to a larger volume of material removal from the electrode, causing accelerated wear. The reduced interaction time between the electrode and the workpiece at higher servo speeds allows for more material to adhere to the electrode surface, further contributing to increased wear. Additionally, the potential reduction in flushing efficiency at higher servo speeds can lead to the re-deposition of eroded material on the electrode, exacerbating the wear.

3.7.4 Perpendicularity

The EDM experiments on Si_3N_4-TiN ceramic composites revealed a significant relationship between servo speed and perpendicularity of the machined features. As the servo speed increased, the perpendicularity reduced simultaneously throughout the servo speed. However, a notable change in the rate of perpendicularity reduction was observed between 5 m/s and 6 m/s, where the reduction rate was relatively low. After 6 m/s, the perpendicularity suddenly reduced at a higher rate.

At higher servo speeds, the material removal rate also increases, as discussed earlier. The higher material removal rate can lead to a higher volume of material being removed from the workpiece, which can influence the perpendicularity of the machined features. The increased material removal can potentially introduce variations and inaccuracies in the machined surface, affecting the perpendicularity.

3.7.5 Cylindricity

The EDM experiments on Si_3N_4-TiN ceramic composites revealed a significant relationship between servo speed and cylindricity of the machined features. The analysis showed that as the servo speed increased, the cylindricity of the machined material initially increased up to 6 m/s. However, beyond 6 m/s, the cylindricity of the machined material started to decrease.

3.7.6 Circularity and Cylindricity

The experimental results suggest that both the cylindricity and circularity of the machined material initially increase up to 6 m/s, indicating an improvement in machining precision and accuracy at these speeds. This improvement can be attributed to improved tool path dynamics, optimal material removal rate, reduced thermal effects, and reduced electrode wear. However, beyond 6 m/s, both the cylindricity and circularity start to decrease, which can be attributed to the influence of dynamic tool path behavior and potential instabilities in the machining process at these high servo speeds. The dynamic effects can introduce errors in the tool motion, leading to deviations from the desired geometrical tolerances.

3.7.7 Run out

The EDM experiments on Si_3N_4-TiN ceramic composites revealed a significant relationship between servo speed and runout of the machined features. As the servo speed increased, the runout reduced simultaneously throughout the servo speed. However, a notable change in the rate of runout reduction was observed between 5 m/s and 6 m/s, where the reduction rate was relatively low. After 6 m/s, the runout suddenly reduced at a higher rate.

At lower servo speeds, the discharge energy may not be as intense, leading to less efficient material removal and potential thermal effects on the workpiece. As the servo speed increases, the discharge energy also increases, leading to more efficient and localized material removal. The higher servo speeds reduce the duration of electrical discharges, which can minimize heat-affected zones and thermal distortion, resulting in reduced runout.

3.7.8 Surface Roughness

It was observed that as the servo speed increased, the surface roughness initially decreased up to 6 m/s, after which it started to increase.

At lower servo speeds (5 m/s), the machining process exhibited relatively poor material removal rates, resulting a surface roughness value of 0.41 µm. As the servo speed was increased to 6 m/s, the material removal rate improved, leading to a reduction in surface roughness. The peak-to-valley distance decreased, and the surface became smoother, indicating better material removal efficiency.

However, beyond the servo speed of 6 m/s, the surface roughness started to increase. This deterioration in surface

finish can be attributed to various factors. First, at higher servo speeds, the discharge energy may have increased excessively, leading to the generation of larger craters and micro-cracks on the machined surface. Second, the excessive thermal energy might have induced localized melting and recasting of the material, resulting in a rougher surface texture.

3.7.9 Radial Overcut, Bottom Diameter, and Top Diameter of the drilled hole

The experimental results revealed an interesting trend with respect to the servo speed. Initially, as the servo speed increased up to 6 m/s, the Radial Overcut, Bottom Diameter, and Top Diameter of the drilled hole increased. However, beyond 6 m/s, these parameters started to decrease.

At lower servo speeds, the thermal energy delivered to the machining zone is relatively low. This results in less efficient material removal, leading to a smaller Radial Overcut and reduced material removal at the bottom and top of the drilled hole. As the servo speed increases, more thermal energy is delivered to the machining zone, enhancing the material removal rate and increasing the Radial Overcut and hole diameters.

Beyond a certain servo speed (6 m/s in this case), the machining process encounters a critical threshold. At higher speeds, excessive thermal energy may be generated, causing overheating of the tool-electrode and the workpiece. This overheating leads to accelerated tool wear, increased electrode erosion, and reduced machining accuracy. Consequently, the Radial Overcut, Bottom Diameter, and Top Diameter start to decrease due to a compromised and less stable EDM process.

3.7.10 Taper Angle

The EDM experiments on Si_3N_4-TiN ceramic composites revealed an interesting relationship between servo speed and the taper angle of the machined circle. The analysis showed that as the servo speed increased, the taper angle of the machined circle reduced suddenly at a high rate from 5 m/s to 6 m/s. After 6 m/s, the taper angle of the machined circle continued to reduce, but at a lower rate.

As the servo speed increases, the electrode wear rate reduces, as discussed earlier. The improved flushing, reduced overcut, higher energy density, shorter discharge durations, and improved surface quality contribute to decreased electrode wear. The reduced electrode wear at higher servo speeds can lead to a more stable and consistent tool shape, resulting in a reduction in taper angle.

3.7.11 Radial Overcut

The EDM experiments on Si_3N_4-TiN ceramic composites revealed a significant relationship between servo speed and radial overcut of the machined features. The analysis showed that as the servo speed increased, the radial overcut reduced simultaneously throughout the entire range of servo speeds.

The increased servo speed leads to more frequent and intense electrical discharges, resulting in a higher energy density at the machining zone. This increased energy density promotes faster and more efficient material removal, reducing the radial overcut.

3.8 Effect of Input Parameters on Surface Quality

In the conducted EDM process on Si_3N_4-TiN ceramic composites, a systematic investigation of various input parameters was carried out to understand their influence on the resultant surface quality. The input parameters included Polarity, Current, Pulse on Time, Pulse Off Time, Dielectric Pressure, Gap Voltage, Spark Gap, and Servo Speed. The analysis of the machined surfaces using a scanning electron microscope revealed distinct surface characteristics based on these input parameters.

The investigation showed a clear trend in surface quality variation based on the order of the input parameters. The surfaces obtained were categorized into three groups: worst, optimal, and smooth. These groups aligned with the range of input parameter values applied during the EDM process.

3.8.1 Worst Surface

The worst surface quality was observed when higher-order input parameters were employed. From the Fig. 11(a) it seems that this phenomenon can be attributed to intensified material removal rates and larger discharge energies. The higher current, longer pulse on time, and shorter pulse off time collectively lead to enhanced thermal energy deposition and more aggressive material removal. Consequently, this results in a rougher surface with increased thermal damage and re-solidified molten material.

3.8.2 Optimal Surface

The medium-order input parameters yielded an optimal surface quality. From the Fig. 11(b) it seems that this can be attributed to a balanced combination of material removal and thermal effects. The chosen parameter values likely led to controlled and efficient removal of material while minimizing excessive thermal damage. The resulting surface exhibited a desirable compromise between material removal rate and surface integrity.

3.8.3 Smooth Surface

Employing lower-order input parameters resulted in the attainment of a smooth surface. Reduced discharge energy,

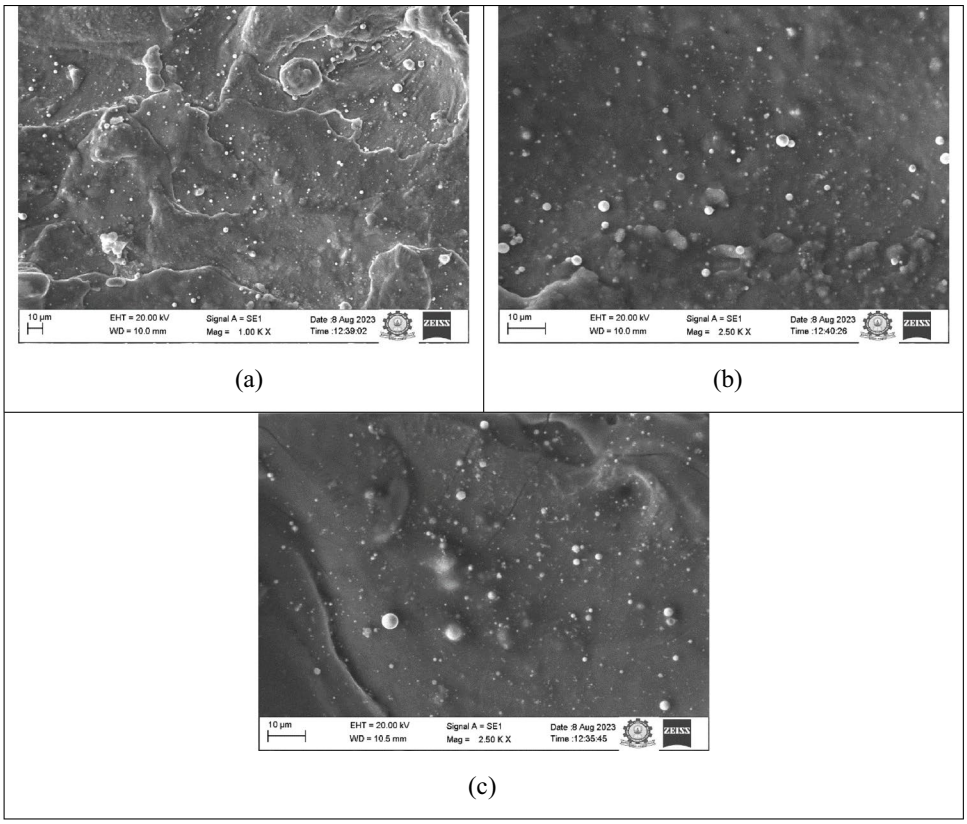

Fig. 11 (**a**) Worst Surface, (**b**) Optimal Surface, (**c**) Smooth Surface

lower current, longer pulse off time, and appropriate gap voltage collectively contributed to gentler material removal. The reduced thermal effects helped maintain surface integrity, leading to a smoother finish as shown in Fig. 11(c).

4 Conclusions

This research endeavour has shed new light on the intricate relationship between input process parameters and the intertwined domains of machining output parameters and geometrical tolerance responses in Wire Electrical Discharge Machining (WEDM) of Si_3N_4 composites.

By delving into the combined effects of polarity, pulse current, pulse on time, pulse off time, dielectric pressure, gap voltage, spark gap, and servo speed, we have not only advanced our understanding of WEDM but also uncovered novel insights. The interplay between these factors has been found to exert a profound influence on critical performance metrics, including metal removal rate, electrode wear, wear ratio, and surface roughness. Equally significant is our revelation that geometrical tolerances, encompassing circularity, cylindricity, perpendicularity, and radial overcut, are intricately intertwined with these output parameters. The conclusion are mentioned below:

1. Material Removal Rate Enhancement: Material Removal Rate (MRR) is an important metric for effective EDM, and the trials showed that it improved significantly when process parameters were chosen with care.
2. Reduced Electrode Wear: The Electrode Wear Rate was significantly reduced due to the optimised the EDM process settings, which meant that the electrodes lasted longer and were replaced less often.
3. Improved Geometric Accuracy: Improvements in Circularity, Cylindricity, and Perpendicularity were seen in the experimentally improved workpiece geometry, which reflects the accuracy that can be achieved using EDM.
4. Hole Diameter Control: In the studies, the Top Diameter and Bottom Diameter of the drilled holes could be controlled precisely, showing that EDM can make holes with the necessary size.
5. Minimized Run-Out: The machined holes maintain improved concentricity and alignment since having minimised Run-Out by fine-tuning the process settings.
6. Taper Angle Management: The results of the trials allowed for precise regulation of the Taper Angle, allowing for the production of holes with almost little variation from the target angle.
7. Surface Finish Enhancement: This capacity to significantly reduce surface roughness via meticulous parame-

ter selection suggests that Si_3N_4-TiN ceramic composites may be used to create smoother surfaces.

8. Practical Implications: Implications for improving EDM processes to achieve targeted quality, efficiency, and cost targets are offered by these results, which have real-world applications in the precise machining of Si_3N_4-TiN ceramic composites.

These results enhance the general precision and efficiency of EDM operations, which makes it a useful tool for sectors requiring precise machining, such aerospace, medical device production, and others that have tight geometrical tolerances. Improved performance and dependability in mission-critical applications are guaranteed by using the recommended best-practice parameter combinations for EDM.

Finally, improving geometric accuracy, surface finish, run-out minimization, electrode wear rates, material removal rates, and taper angle management through systematic optimisation of EDM process parameters for Si_3N_4-TiN ceramic composites yields useful insights for precision machining applications across industries.

Acknowledgements Not Applicable.

Author Contributions Manikandan—Drafted the full manuscript.
Thirugnanam—Supervised and Reviewed the data and full manuscript.
Selvarajan—Analysis and Prepared the figures and table.
Senthilkumar—Analysis and Reviewed the full manuscript.

Funding The authors declare that no funds, grants, or other support were received during the preparation of this manuscript.

Data Availability No datasets were generated or analysed during the current study.

Code Availability Not applicable.

Declarations

Competing Interests The authors declare no competing interests.

Ethics Approval For ethics approval, plagiarism report for this peak current paper has been attached. And its result is 8% similarity.

Consent to Participate Informed consent was obtained from all individual participants included in the study.

Consent for Publication I understand that the text and any pictures or videos published in the article will not be used anywhere.

References

1. Selvarajan L, Sathiya Narayanan C, JeyaPaul R (2016) Optimization of EDM parameters on machining Si_3N_4–TiN composite for improving circularity, cylindricity, and perpendicularity. Mater Manuf Processes 31(4):405–412. https://doi.org/10.1080/10426914.2015.1058947
2. Muthuramalingam T, Mohan B, Vignesh S (2018) Performance Analysis of Pulse Generators on Residual Stress of Machined Silicon Steel Using the EDM Process. SILICON 10:1785–1792. https://doi.org/10.1007/s12633-017-9671-5
3. Rahul MDK, Datta S et al (2018) Effects of Tool Electrode on EDM Performance of Ti-6Al-4V. SILICON 10:2263–2277. https://doi.org/10.1007/s12633-018-9760-0
4. Selvarajan L, Manohar M, Amos Robert J, Jayachandran MP, Selvakumar P (2018) A review on less tool wear rate and improving surface quality of conductive ceramic composites by spark EDM. Materials Today: Proceedings 5(2):5774–5782. https://doi.org/10.1016/j.matpr.2017.12.174
5. Daneshmand S, Masoudi B (2018) Investigation of Weight Percentage of Alumina Fiber on EDM of Al/Al_2O_3 Metal Matrix Composites. SILICON 10:1003–1011. https://doi.org/10.1007/s12633-017-9562-9
6. Murugan C, Kumar RMS, Alagarsamy SV (2022) Investigations on Electric Discharge Machining Behaviour of Si_3N_4 -TiN Ceramic Composite. SILICON 14:547–555. https://doi.org/10.1007/s12633-020-00848-w
7. Reddy M, Chaitanya K, Venkata R, Gamini S (2021) An experimental investigation and optimization of energy consumption and surface defects in wire cut electric discharge machining. Journal of Alloys and Compounds 861:158582. https://doi.org/10.1016/j.jallcom.2020.158582
8. Selvarajan L, Rajavel R, Prakash B, Mohan Dhanesh G, Gopi S (2020) Investigation on spark electrical discharge machining of Si3N4 based advanced conductive ceramic composites. Materials Today: Proceedings 27:2174–2178. https://doi.org/10.1016/j.matpr.2019.09.090
9. Selvarajan L, Rajavel J, Prabakaran V, Sivakumar B, Jeeva G (2018) A review paper on EDM parameter of composite material and industrial demand material machining. Materials Today: Proceedings 5(2):5506–5513
10. Srinivasan VP, Palani PK, Selvarajan L (2018) Experimental investigation on electrical discharge machining of ceramic composites (Si_3N_4-TiN) using RSM. Int J Comput Mater Sci Surf Eng 7(2):104–115
11. Srinivasan VP, Palani PK, Balamurugan S (2021) Experimental investigation on EDM of Si3N4–TiN using grey relational analysis coupled with teaching-learning-based optimization algorithm. Ceram Int 47(13):19153–19168. https://doi.org/10.1016/j.ceramint.2021.03.262
12. Kumar SS, Erdemir FATİH, Temel Varol, Thirumalai Kumaran S, Uthayakumar M, Aykut Canakci (2020) Investigation of WEDM process parameters of Al–SiC–B4C composites using response surface methodology. International Journal of Lightweight Materials and Manufacture 3 (2):127–135. https://doi.org/10.1016/j.ijlmm.2019.09.003
13. Senthil Kumar S, Sudhakara Pandian R, Pitchipoo P, Senthilkumar TS, Ponnambalam SG (2022) Investigation of Wear and Wire Electrical Discharge Machining Characteristics of Al-Mg-MoS 2 Composites Using Response Surface Method. J Test Eval 51:2
14. Charfi A, Aziz R, Kharrat M, Wani MF, Dammak M, Sehgal R (2022) Friction and wear characterization of nanocomposites based on Si3N4 reinforced with SiC, Mo, MoSi2 nanoparticles. Trans Indian Inst Met 75:855–865. https://doi.org/10.1007/s12666-021-02494-1
15. Petrovic JJ (1995) Mechanical Behavior of MoSi2 and MoSi2 Composites. Mater Sci Eng A 192:31–37. https://doi.org/10.1016/0921-5093(94)03246-7
16. Gao JY, Jiang W (2009) Effect of La2O3 Addition to Modification of Grain-Boundary Phase in MoSi2. J Alloys Compd 476(1–2):667–670. https://doi.org/10.1016/j.jallcom.2008.09.076
17. Zakeri M, Ramezani M (2012) Synthesis of MoSi2-TiC Nanocomposite Powder via Mechanical Alloying and Subsequent Annealing.

Ceram Int 38(2):1353–1357. https://doi.org/10.1016/j.ceramint.2011.09.012
18. Selvarajan L, Sathiya Narayanan C, Jeyapaul R (2015) Optimization of Process Parameters to Improve Form and Orientation Tolerances in EDM of MoSi2-SiC Composites. Mater Manuf Process 30(8):954–960. https://doi.org/10.1080/10426914.2014.962041
19. Shabgard MR, Gholipoor A, Mohammadpourfard M (2019) Investigating the Effects of External Magnetic Field on Machining Characteristics of Electrical Discharge Machining Process, Numerically and Experimentally. Int J Adv Manuf Technol 102(1–4):55–65. https://doi.org/10.1007/s00170-018-3167-3
20. Wang P, Li B, Shi G, Lin T, Wang B (2018) Non-Linear Mechanism in Electrical Discharge Machining Process. Int J Adv Manuf Technol 97(5–8):1687–1696. https://doi.org/10.1007/s00170-018-1888-y
21. Singh B, Kumar S, Kumar J (2017) Multi-objective optimization in electrical discharge machining of 6061 Al/SiCp using RSM and NSGA-II. In: Key Engineering Materials. Trans Tech Publications, Ltd., vol 748, pp 207–211. https://doi.org/10.4028/www.scientific.net/KEM.748.207
22. Senthilkumar TS, Muralikannan R, Ramkumar T, Senthil KS (2021) Studies of kerf width and surface roughness using the response surface methodology in AA 4032–TiC composites. Proceedings of the Institution of Mechanical Engineers, Part E: Journal of Process Mechanical Engineering 235(6):2240–2253. https://doi.org/10.1177/09544089211041418
23. Alduroobi AAA, Ubaid AM, Tawfiq MA, Elias RR (2020) Wire EDM process optimization for machining AISI 1045 steel by use of Taguchi method, artificial neural network and analysis of variances. Int J Syst Assur Eng Manag 11(6):1314–1338
24. Panda MR, Panda SS, Narang HK(2020) Multi-objective optimization of Al–Al2O3 MMC during electro discharge machining using desirability function approach. In: Li L, Pratihar D, Chakrabarty S, Mishra P (eds) Advances in Materials and Manufacturing Engineering. Lecture Notes in Mechanical Engineering. Springer, Singapore, pp 485–493. https://doi.org/10.1007/978-981-15-1307-7_55
25. Senthilkumar ST, Senthil Kumar S, Vignesh Kumar V, Rathinavel S, Selvarajan L, Nagaprasad N (2022) Worn surface analysis and wear map mechanism of AA4032 composites. J Test Eval 51(2):1151–1165. https://doi.org/10.1520/JTE20220149
26. Machno M, Matras A, Szkoda M (2022) Modelling and Analysis of the Effect of EDM-Drilling Parameters on the Machining Performance of Inconel 718 Using the RSM and ANNs Methods. Mater 15(3):1152
27. Senthilkumar TS, Senthil KS, Rathinavel S (2023) Performance analysis of conventional and DMLS copper electrode during eDM process in AA4032-TiC composite. 3D Print Addit Manuf 10(3):569-583. https://doi.org/10.1089/3dp.2021.0030
28. Chaudhari R, Vora J, Parikh DM, Wankhede V, Khanna S (2020) Multi-response optimization of WEDM parameters using an integrated approach of RSM–GRA analysis for pure titanium. J Inst Eng India Ser D 101:117–126. https://doi.org/10.1007/s40033-020-00204-7
29. Senthil Kumar S, Sudhakara Pandian R, Pitchipoo P, Narayanasamy P, Senthilkumar TS (2022) Surface and subsurface investigation of Al-Mg-MoS2 composite on performing wire electrical discharge machining. Surf Topogr Metrol Prop 10(1):015047
30. Senthilkumar TS, Muralikannan R (2019) Role of TiC and h-BN particles on morphological characterization and surface effects of Al 4032 hybrid composites using EDM process. J Mech Sci Technol 33:4255–4264. https://doi.org/10.1007/s12206-019-0822-z
31. Selvarajan L, Rajavel R, Nair A, Chandrasekaran M (2023) Testing and Evaluation of the Spark Erosion Parameter for Machining Intermetallic Ceramic Composite for Enhancing Drilled Hole Accuracy. J Test Eval 52(1):20220685–20220685. https://doi.org/10.1520/jte20220685
32. Selvarajan L, Venkataramanan K (2023) Surface morphology and drilled hole accuracy of conductive ceramic composites Si_3N_4–TiN and $MoSi_2$–SiC on EDMed surfaces. Wear 530–531:204973–204973. https://doi.org/10.1016/j.wear.2023.204973
33. Selvarajan L, Venkataramanan K, Choudhury B, Chandrasekaran M (2024) Evaluating of surface morphology on EDD machining parameters for Si_3N_4-TiN using TLBO-MRA. Mater Manuf Process 39(4):465–479. https://doi.org/10.1080/10426914.2023.2219307
34. Selvarajan L, Venkataramanan K (2024) Evaluations of surface morphology in EDMed $MoSi_2$-SiC intermetallic ceramic composite surfaces. J Adhes Sci Technol 38(2):225–247. https://doi.org/10.1080/01694243.2023.2225250
35. Selvarajan L, Venkataramanan K, Rajavel R, Senthilkumar TS (2023) Fuzzy logic optimization with regression analysis on EDM machining parameters of Si_3N_4-TiN ceramic composites. Journal of Intelligent and Fuzzy Systems 44(6):8869–8888. https://doi.org/10.3233/jifs-223650
36. Selvarajan L, Rajavel R, Arun C, Raju C (2023) Experimental Analysis and Surface Morphology of Holes Made by Electrical Discharge Machining on MoSi2-SiC Composite. J Mater Eng Perform. https://doi.org/10.1007/s11665-023-09000-2
37. Selvarajan L, Rajavel R, Venkataramanan K, Srinivasan V (2023) Experimental investigation on surface morphology and recasting layer of Si_3N_4-TiN composites machined by die-sinking and rotary EDM. Ceram Int 49(5):8487–8501. https://doi.org/10.1016/j.ceramint.2022.11.011
38. Lakshmanan S, Rajendran R, Shanmugakani SK, Krishnamoorthy V. (2023) Analyzing the geometrical errors of silicon nitride-titanium nitride on performing electric discharge machining using response surface methodology. Proceedings of the Institution of Mechanical Engineers, Part E: Journal of Process Mechanical Engineering 0(0). https://doi.org/10.1177/09544089231166303